completely overlapped, as shown in Figure 7. The parameters for the tetrahedral iron [$\delta = 0.18$ and $\Delta E_q = 1.16$ mm s^{-1} (293 K); $\delta = 0.30$ and $\Delta E_q = 1.22$ mm s^{-1} (50 K)] are assigned by comparison with the symmetrical $[Cl_3FeOFeCl_3]^{2-}$ complex.[7] For the octahedral iron the isomer shift [$\delta = 0.29$ (293 K) and 0.40 mm s^{-1} (50 K)] is at the bottom end of the range observed for symmetrical bisoctahedral (μ-oxo)diiron(III) systems.[22] This low value is attributed to perturbation from the $OFeCl_3$ moiety. Similar behavior was observed for the N5 analogues.[5b] The large values for the quadrupole splitting [$\Delta E_q = 1.40$ (293 K) and 1.41 mm s^{-1} (50 K)] are typical of other (μ-oxo)diiron(III) systems and are not significantly different from that for $[N5FeOFeCl_3]Cl$, at least at 293 K—at low temperatures (50 and 77 K, respectively) the Mössbauer spectra are visibly different, with $[N5FeOFeCl_3]Cl$ having perfectly overlapped quadrupole doublets at 77 K.[5b]

Conclusions

In the unsymmetrical complexes, $[NmFeOFeCl_3]^+$, where Nm provides five nitrogenous ligands to the iron center, the lowered symmetry, C_s, combined with the comparable ligand orbital energies around the dissimilarly coordinated iron centers leads to stronger antiferromagnetic coupling ($-J > 120$ cm^{-1}) than is seen in symmetrical singly bridged species with higher symmetry, C_{2v}. Also characteristic of these unsymmetrical molecular structures is the observation in the infrared spectrum of a strong doublet at ca. 850, 835 cm^{-1} associated with the Fe–O–Fe′ group and in the resonance Raman spectrum of a value greater than unity for the ratio of the intensities of the asymmetric to the symmetric Fe–O–Fe stretch.

Acknowledgment. We gratefully acknowledge the support of the National Institute of Diabetic, Kidney, and Digestive Diseases of the National Institutes of Health through Grant 5 R01 DK37702 (G.B.J.), the Solid State Chemistry Program of the National Science Foundation through Grant DMR 8313710 (W.M.R.), and the Comite Conjunto Hispano-Norteamericano para la Cooperacion Cultural y Educativa for a fellowship to P.G.-R. We thank Dr. Joann Sanders-Loehr and Jinshu Ling for the resonance Raman spectrum, Dr. Ekk Sinn and Dr. Thitinant Thanyasiri for the collection of magnetic susceptibility data, and Dr. Nieves Casaon-Pastor and Dr. Nancy Morris for recording the NMR spectra.

Registry No. $N_6 \cdot HCl$, 129240-50-2; $[N_6FeOFeCl_3]Cl \cdot 3H_2O \cdot 2CH_3OH \cdot 0.5HCl$, 129264-58-0.

Supplementary Material Available: Tables of full crystal and refinement data (Table S-I), atomic and isotropic thermal parameters (Table S-II), anisotropic displacement parameters (Table S-III), bond distances (Table S-IV), bond angles (Table S-V), torsion angles (Table S-VI), and rms amplitudes of anisotropic displacement (Table S-VII) and a unit cell diagram (Figure S-1) (12 pages); a listing of structure factors (43 pages). Ordering information is given on any current masthead page.

---

[22] Gibb, T. C.; Greenwood, N. N. In *Mössbauer Spectroscopy*; Chapman and Hall: London, 1971.

Contribution from the Institute of Inorganic Synthesis,
Yamanashi University, Miyamae-cho 7, Kofu, 400 Japan

Preparation of an Acid Niobium Phosphate and Alkali-Metal Niobium Phosphates, Having $NbOPO_4 \cdot H_2O$ Layers Condensed with the Phosphate Group

Nobukazu Kinomura* and Nobuhiro Kumada

Received May 1, 1990

New alkali-metal niobium phosphates and an acid niobium phosphate were prepared under low temperature hydrothermal conditions. Their chemical formulas were deduced to be $NaNb_2(OH)_2(PO_4)_3 \cdot 2.5H_2O$, $KNb_2(OH)_2(PO_4)_3 \cdot nH_2O$, and $HNb_2(OH)_2(PO_4)_3 \cdot H_2O$, having lattice constants of $a = 6.488$ (2) Å and $c = 16.286$ (5) Å in the tetragonal system, $a = 6.489$ (3) Å, $b = 6.452$ (2) Å, $c = 16.149$ (6) Å, and $\beta = 95.63$ (3)° in the monoclinic system, and $a = 6.485$ (2) Å, $b = 6.415$ (3) Å, $c = 16.18$ (2) Å, $\alpha = 90.11$ (7)°, $\beta = 95.91$ (5)°, and $\gamma = 90.95$ (5)° in the triclinic system, respectively. They are isostructural, having a three-dimensional structural framework composed of $NbO(H_2O)(PO_4)$ layers combined with PO_4 groups. The alkali-metal ions and protons are exchangeable with other alkali-metal, alkaline-earth-metal, and alkylammonium ions. The acid niobium phosphate can intercalate n-alkylamines. The PO_4 group that links the layers is removed upon ion exchange with certain ions and upon intercalation with certain amines, and the three-dimensional structure is transformed to a layered structure.

Introduction

Vanadium phosphate shows a reversible change from an anhydrous three-dimensional structure for α-$VOPO_4$ to hydrated layered structures for $VOPO_4 \cdot nH_2O$.[1] The crystal structure of $VOPO_4 \cdot 2H_2O$, which was analyzed by Teitze,[2] consists of layers of $VO_5(H_2O)$ octahedra and PO_4 tetrahedra that share corners and water molecules in the interlayer spaces connecting the layers. In the system Nb_2O_5–P_2O_5–H_2O, similar anhydrous and hydrated niobium phosphates were reported,[3-5] but the change from hydrated phase to dehydrated phase was irreversible.

Beneke and Lagaly[6] reported that $NbOPO_4 \cdot nH_2O$ can intercalate various types of amines in the interlayer spaces. Niobium phosphates that contain neutral acid molecules H_3PO_4 and H_2SO_4 and water molecules in the interlayer spaces were also prepared, but the acid was removed with ease by washing with water.[6,7] Beneke and Lagaly[6] also mentioned preparation of the layered acid niobium phosphate $Nb_2(OH)_2(HPO_4)(PO_4)_2 \cdot 4.4H_2O$, which is composed of two layers of $Nb(OH)_2PO_4$ connected by the PO_4 group, as if the neutral H_3PO_4 intercalated into the interlayer spaces condensed to link the layers.

We report here the preparation of alkali-metal niobium phosphates and an acid niobium phosphate with three-dimensional structures and their ion-exchange and intercalation behaviors.

Experimental Section

Preparation. Two kinds of starting material were used in this study: amorphous niobium oxide and sodium polyniobate, $Na_8Nb_6O_{19} \cdot 13H_2O$. The preparative method for $Na_8Nb_6O_{19} \cdot 13H_2O$ was described elsewhere.[8] The amorphous starting material was prepared by fusing niobium pentaoxide with K_2CO_3, dissolving in water, and precipitating with hydro-

---

[1] Ladwig, G. *Z. Anorg. Allg. Chem.* **1965**, *338*, 266.
[2] Tietze, H. R. *Aust. J. Chem.* **1981**, *34*, 2035.
[3] Longo, J. M.; Kierkegaad, P. *Acta Chem. Scand.* **1966**, *20*, 72.
[4] Levin, E. M.; Roth, R. *J. Solid State Chem.* **1970**, *2*, 250.
[5] Deulin, G. I.; Dushin, R. B.; Krylov, V. N. *Russ. J. Inorg. Chem.* (*Engl. Transl.*) **1979**, *24*, 1291.
[6] Beneke, K.; Lagaly, G. *Inorg. Chem.* **1983**, *22*, 1503.
[7] Chernorukov, N. G.; Egorov, N. P.; Kutsepin, V. F. *Russ. J. Inorg. Chem* (*Engl. Transl.*) **1979**, *24*, 987.
[8] Kinomura, N.; Kumada, N.; Muto, F. *Mater. Res. Bull.* **1984**, *19*, 299.

0020-1669/90/1329-5217$02.50/0 © 1990 American Chemical Society

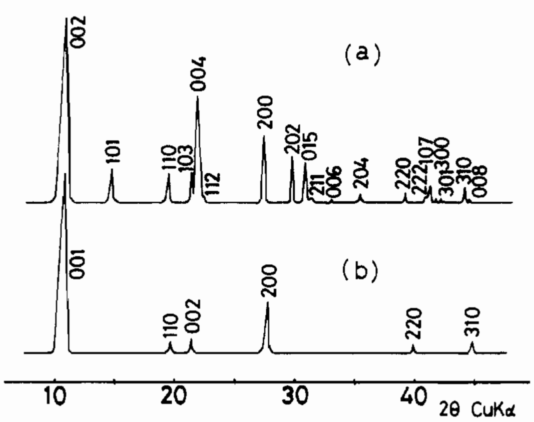

Figure 1. XRD patterns of $NaNb_2(OH)_2(PO_4)_3{\cdot}2.5H_2O$ (a) and $NbOPO_4{\cdot}3H_2O$ (b).

chloric acid. After the precipitate was washed well with distilled water until the pH of the washing water reached about 7, it was dried in air.

Various amounts of the sodium polyniobate (from 0.3 to 3.0 g) were put into an autoclave (17 cm^3 in volume) together with 6 cm^3 of phosphoric acid (85 wt %). The autoclave was heated at temperatures ranging from 100 to 200 °C for 5 days to 3 weeks in an oil bath. Preparation by using the amorphous starting material was attempted for the system including Li^+, K^+, or no alkali-metal ions. A 0.7-g sample of starting material was treated with KOH or $LiOH{\cdot}H_2O$ in a mixture of phosphoric acid and water under the same hydrothermal conditions as in the previous preparation. Several variants as to the amount of the alkali-metal hydroxide, the ratio of phosphoric acid and water, and the temperature were tried. The products were separated by centrifuging, washed with distilled water several times, and dried in air.

Ion Exchange. Ion-exchange properties were examined by using 0.1 M chloride solutions of other alkali-metal, alkaline-earth-metal, Ni^{2+}, and Zn^{2+} ions as well as *n*-alkylammonium ions. The ion-exchange reaction was carried out at 60 and 90 °C for up to 2 weeks, and the product was separated by centrifuging. The acid niobium phosphate was reacted with pure *n*-alkylamines at room temperature. The product containing sodium was also treated with 0.5 M acids under the same conditions as for the ion exchange.

Characterization. The products were identified by X-ray powder diffraction (XRD) using Ni-filtered Cu Kα radiation. The lattice constants were determined by least-squares refinement of powder patterns recorded with a scanning speed of 0.25°/min by using silicon as an internal standard. Thermal variation of the lattice constants was followed by XRD up to 550 °C. Density was measured by using a pycnometer.

Differential thermal analysis (DTA) and thermogravimetry (TG) were measured with a heating rate of 10 °C/min up to 1000 °C. Chemical composition was analyzed by the X-ray fluorescence analysis. The ion-exchange rate was determined by analyzing sodium ions released into the solution by atomic absorption spectroscopy. In the course of the experiment phosphoric acid was occasionally found to be released into the solution on ion exchange, and in these cases the amount of phosphorus was analyzed by inductively coupled plasma emission spectroscopy (ICP).

Results

Synthesis of $NaNb_2(OH)_2(PO_4)_3{\cdot}2.5H_2O$. Several new compounds appeared in the systems Na_2O–Nb_2O_5–P_2O_5–H_2O and Nb_2O_5–P_2O_5–H_2O, depending mainly on the concentration of phosphoric acid. Their XRD patterns were indexed with tetragonal unit cells and the *a* axes were very similar to each other as well as to that of $NbOPO_4{\cdot}nH_2O$. Among them, the compound that was prepared in the region poor in phosphoric acid will be reported in detail here.

The optimum conditions for preparation of the compound from $Na_8Nb_6O_{19}{\cdot}13H_2O$ were the following: the starting ratio of constituents was Na:Nb:P = 4:3:28, the temperature was 150 °C, and the reaction time was longer than 1 week. When phosphoric acid became poorer than in the region for this compound, perovskite-type or (and) ilmenite-type $NaNbO_3$ was obtained.[8] The same compound was obtained under similar conditions from the amorphous starting material and NaOH.

Characterization. The XRD pattern of the product is shown in Figure 1, together with that of $NbOPO_4{\cdot}3H_2O$, and the XRD data are listed in Table I. The pattern was completely indexed with a tetragonal cell of $a = 6.488$ (2) Å and $c = 16.286$ (5) Å. Chemical analysis revealed the chemical formula of the product to be $NaNb_2(OH)_2(PO_4)_3{\cdot}2.5H_2O$. Anal. Calcd: Na_2O, 5.4; Nb_2O_5, 46.4; P_2O_5, 37.2; H_2O, 11.0 Found: Na_2O, 5.2; Nb_2O_5, 48.9; P_2O_5, 36.0; H_2O, 10.9. The observed density of 2.77 g/cm^3 indicated two formula units per unit cell ($d_{calcd} = 2.775$ g/cm^3).

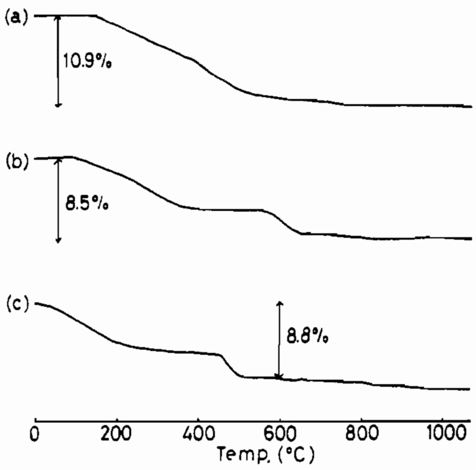

Figure 2. TG curves of the alkali-metal niobium phosphates and the acid niobium phosphate: (a) $NaNb_2(OH)_2(PO_4)_3{\cdot}2.5H_2O$; (b) $KNb_2(OH)_2(PO_4)_3{\cdot}nH_2O$ (measured probably with small amount of amorphous substance); (c) $HNb_2(OH)_2(PO_4)_3{\cdot}H_2O$.

In the DTA curve of the product, broad endothermic peaks were observed at about 120 and 370 °C, accompanied by a continuous weight loss up to about 450 °C, as shown in the TG curve in Figure 2. At 750 °C a sharp exothermic peak was observed, and above this temperature $NbOPO_4$ was the only crystalline phase seen in the XRD pattern. Although splitting of the 101 reflection was observed at 100 °C and then a monoclinic cell with $a = 6.46$ Å, $b = 6.48$ Å, $c = 16.2$ Å, and $\beta = 92.8°$ was obtained, a high-temperature XRD study revealed that the *a* axis (and *b* axis) continuously decreased a little. On the other hand, the *c* axis, which had remained unchanged up to 300 °C, shrank abruptly by about 1 Å between 300 and 400 °C. These observations indicate that the water molecules removed below about 300 °C are zeolitic water and that protons are removed as water at higher temperatures. No decrease in the *c* axis upon removal of water molecules implies that the structure of this compound is a three-dimensional one, unlike that of $NbOPO_4{\cdot}nH_2O$.

Preparation of Isomorphous Compounds. In the systems K_2O–Nb_2O_5–P_2O_5–H_2O and Nb_2O_5–P_2O_5–H_2O, potassium niobium phosphate and the acid niobium phosphate isostructural with $NaNb_2(OH)_2(PO_4)_3{\cdot}2.5H_2O$ were found to be prepared as almost single phases from their XRD. The optimum ratios of constituents are K:Nb:P = 4:1:28 and Nb:P:H$_2$O = 1:10:50. In the system K_2O–Nb_2O_5–P_2O_5–H_2O, the product showed only a rather broad XRD pattern, even after a month at 150 °C, and chemical analysis was not attempted. However from the resemblance of the XRD pattern to that of the sodium niobium phosphate, the chemical formula for this compound was deduced to be $KNb_2(OH)_2(PO_4)_3{\cdot}nH_2O$. Chemical analysis of the acid niobium phosphate gave the formula of $HNb_2(OH)_2(PO_4)_3{\cdot}H_2O$ for the acid niobium phosphate obtained in the system Nb_2O_5–P_2O_5–H_2O. Anal. Calcd: Nb_2O_5, 50.6; P_2O_5, 40.5; H_2O, 8.9. Found: Nb_2O_5, 51.3; P_2O_5, 39.1; H_2O, 8.8. In the system Li_2O–Nb_2O_5–P_2O_5–H_2O, the product was composed of two phases, of which the XRD patterns are very similar to each other, to the other hydrated alkali-metal niobium phosphates, and to $NbOPO_4{\cdot}3H_2O$. From their high-temperature behavior one of them was found to have a layered structure while the other was found to have a three-dimensional one similar to that of the other hydrated alkali-metal niobium phosphates.

Ion Exchange with Metal Ions. More than 50% of the sodium ions were exchanged (or extracted) with 0.1 M alkali-metal and alkaline-earth-metal ions and protons at 60 °C in 2 weeks (Table IIa). The *a* axis was almost unaffected by the exchange, but the *c* axis varied with some of the ions. Changes in the *c* axis were

Table I. XRD Data of Sodium Niobium Phosphate (a), Potassium Niobium Phosphate (b), and the Acid Niobium Phosphate (c)[a]

a				b				c			
hkl	d_{calcd}	d_{obs}	I/I_0	*hkl*	d_{calcd}	d_{obs}	I/I_0	*hkl*	d_{calcd}	d_{obs}	I/I_0
002	8.14	8.14	100	002	8.04	8.04	100	002	8.05	8.03	100
101	6.03	6.03	18	$10\bar{1}$	6.21	6.21	2	$10\bar{1}$	6.21	6.21	5
110	4.59	4.59	16	101	5.80	5.78	2	101	5.78	5.79	6
103	4.16	4.17	16	110	4.56	4.59	2	$1\bar{1}0$	4.59	4.59	7
004	4.07	4.07	57	$10\bar{3}$	4.34	4.35	1	110	4.51	4.53	4
112	4.00	4.00	3	004	4.02	4.02	59	$10\bar{3}$	4.35	4.35	3
200	3.244	3.244	36	103	3.94	3.93	2	004	4.02	4.02	57
202	3.014	3.014	24	200	3.23	3.23	9	103	3.93	3.93	6
105	2.911	2.912	22	$20\bar{1}$	3.23			200	3.227	3.225	29
211	2.857	2.856	2	202	3.23			020	3.207	3.204	5
006	2.714	2.713	1	$20\bar{2}$	3.103	3.101	4	$20\bar{2}$	3.106	3.107	11
204	2.537	2.538	4	$10\bar{5}$	2.997	3.002	4	$10\bar{5}$	3.007	3.004	8
220	2.294	2.295	5	$20\bar{3}$	2.894	2.891	1	202	2.893	2.892	4
222	2.208	2.209	3	023	2.764	2.766	2	105	2.769	2.765	4
107	2.190	2.190	8	203	2.653	2.653	1	122	2.648	2.651	2
301	2.144	2.144	1	$20\bar{5}$	2.399	2.397	1	$1\bar{2}\bar{4}$	2.400	2.397	1
310	2.052	2.052	7	$12\bar{4}$	2.394			$1\bar{2}4$	2.302	2.299	2
008	2.036	2.036	1	106	2.393			025	2.268	2.265	3
303	2.009	2.009	3	124	2.297	2.300	1	214	2.236	2.236	2
312	1.990	1.990	3	025	2.277	2.265	1	107	2.099	2.096	4
118	1.861	1.860	2	214	2.253			$3\bar{1}0$	2.049	2.046	2
217	1.815	1.815	3	221	2.238	2.237	1	215	2.046		
305	1.802	1.802	3	$22\bar{2}$	2.236			$3\bar{1}\bar{2}$	2.033	2.031	3
109	1.743	1.743	3	$10\bar{7}$	2.234			$22\bar{4}$	2.033		
323	1.708	1.708	1	107	2.099	2.097	2	$1\bar{3}\bar{1}$	2.031		
400	1.622	1.622	4	$31\bar{1}$	2.049	2.050	1	$1\bar{3}1$	2.012	2.010	2
402	1.591	1.591	3	223	2.049			008	2.012		
325	1.575	1.575	1	$22\bar{4}$	2.046			$1\bar{2}\bar{6}$	2.010		
				$13\bar{1}$	2.032	2.031	1	$21\bar{7}$	1.880	1.879	1
				302	2.030			$30\bar{5}$	1.880		
								$1\bar{3}\bar{4}$	1.841	1.841	1
a = 6.488 (2) Å c = 16.286 (5) Å				a = 6.489 (2) Å b = 6.452 (2) Å c = 16.149 (6) Å β = 95.63 (3)°				a = 6.485 (2) Å b = 6.415 (3) Å c = 16.18 (2) Å α = 90.11 (7)° β = 95.91 (5)° γ = 90.95 (5)°			

[a] *d* spacings are given in angstroms.

Table II. Ion Exchange of Sodium Niobium Phosphate with Metal Ions (a) and with *n*-Alkylamines (b)

(a) Metal Ions

ions	degree of exchange, %	removed P,[a] %	*c* axis, Å
Li^+	40.7	5.4	15.52
Na^+			16.286
K^+	74.5	2.8	16.00
Rb^+	79.4	3.0	15.79
Cs^+	76.6	3.3	15.79
Mg^{2+}	78.0	15.9	18.40
Ca^{2+}	71.4	15.0	18.64
Sr^{2+}	83.6	9.4	18.22
Ba^{2+}	71.8	3.3	16.08
Ni^{2+}	73.3		19.00
Zn^{2+}	70.2		18.40

(b) *n*-Alkylamines

n-alkylamine	degree of exchange, %	removed P,[a] %	*c* axis, Å	*c* axis,[b] Å (intercalation)
methyl	80.1	1.4	16.05	16.10
ethyl	72.8	1.7	16.14	16.15
propyl	40.3	2.2	16.29	16.24
butyl	20.1	3.2	16.31	16.25
hexyl	59.4	10.3	21.8	18.2
octyl	77.8	13.2	26.5	20.8
dodecyl	87.8	11.9	37.0	28.6

[a] Removed amount of P upon ion exchange. [b] The *c* axis of intercalation compounds of pure amines to the acid niobium phosphate.

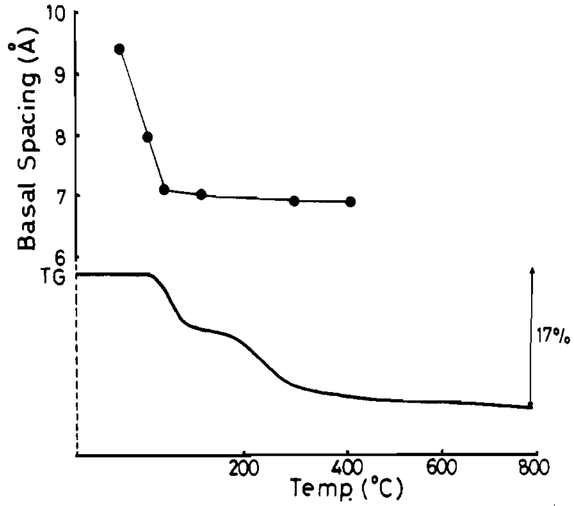

Figure 3. TG curves and change of the basal spacing ($c/2$) for the Sr derivative as a representative of the second-group derivative.

not large upon the ion exchange with other alkali-metal ions and protons, but expansions of the axis were observed by the ion exchange with Ni^{2+}, Zn^{2+}, and alkaline-earth-metal ions, except Ba^{2+}. The XRD patterns of the potassium and proton derivatives were almost identical with those of the potassium niobium phosphate and acid niobium phosphate mentioned above. From this change of the *c* axis upon ion exchange, the exchanged derivatives are divided into two groups: the first group, which includes ion-exchange derivatives of alkali-metal ions, Ba^{2+}, and protons, does not show any change, while the second group shows an expansion. No significant difference in the degree of ion exchange for Na^+ was seen between the two groups. Another characteristic difference between the two groups was seen in their

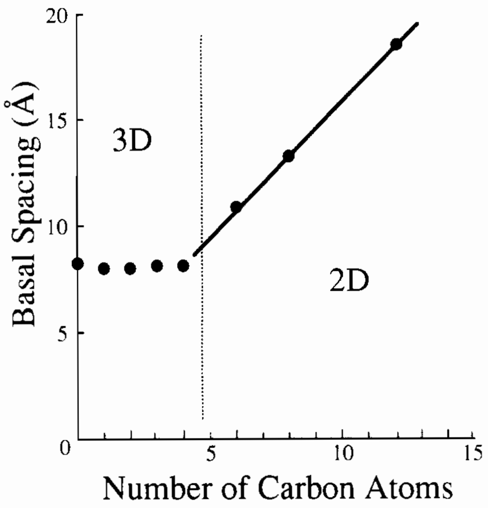

Figure 4. Evolution of the basal spacing ($c/2$, Å) on ion exchange of $NaNb_2(OH)_2(PO_4)_3{\cdot}2.5H_2O$ with alkylammonium ions ($C_mH_{2m+1}NH_3^+$). (2D and 3D mean two-dimensional and three-dimensional structures.)

high-temperature behavior. The first group shows TG–DTA curves and changes of the c axis on heating that are similar to those of the original compound. Unlike the three-dimensional original compound and the first group, the second group exhibits characteristics of layered compounds: a large shrinkage of the c axis upon removal of water at around 100 °C (Figure 3). The decrease of the c axis and weight loss above 300 °C observed for the original compound and the first group does not occur in the second group. The three-dimensional structure was therefore changed to a two-dimensional structure upon ion exchange for the second group.

Prolonged ion exchange or exchange with concentrated solutions resulted in the formation of a mixture of the two groups even for the first-group ions. Especially, extensive treatment of the compound with acids was found, from an XRD pattern and thermal behavior, to produce $NbOPO_4{\cdot}nH_2O$. It is obvious that acids extract not only sodium ions but also phosphate groups from the structure.

As shown by the titration of $HNb_2(OH)_2(PO_4)_3{\cdot}H_2O$ with NaOH, protons in the acid niobium phosphate are exchangeable. The exchanged derivatives from the acid niobium phosphate had lattice constants similar to and upon heating showed behavior similar to those of the corresponding derivatives prepared by ion exchange of sodium niobium phosphate.

Ion Exchange with *n*-Alkylammonium Ions. The results of ion exchange with *n*-alkylammonium ions ($C_mH_{2m+1}NH_3^+$) indicate clearly the difference between the two groups. The degrees of ion exchange and the c axes for the ion-exchanged derivatives are listed in Table IIb. The a axis was almost unaltered upon the exchange, while the c axis dimension was dependent on m. Up to $m = 4$, the c axes were similar to each other as well as to the original compound, and the degree of exchange decreased from 80.1 to 20.1% with an increase of the carbon number. At $m = 6$, the c axis begins to increase with m, as seen in Figure 4, and the degree of exchange increases again. At the same time a considerable amount of phosphorus was removed into the solution in the region of $m \geq 6$, as shown in Table IIb. In the region of $m \leq 4$, the exchanged derivatives belong to the first group where the three-dimensional structure is preserved, while the derivatives with $m \geq 6$ have a layered structure similar to that of the second group.

Unlike those of $NaNb_2(OH)_2(PO_4)_3{\cdot}2.5H_2O$, XRD patterns of $KNb_2(OH)_2(PO_4)_3{\cdot}nH_2O$ and $HNb_2(OH)_2(PO_4)_3{\cdot}H_2O$ could be indexed with a monoclinic cell and a triclinic cell, respectively. XRD patterns and TG curves for these compounds are given in Table I and Figure 2. The change in their c axes on heating was very similar to that of $NaNb_2(OH)_2(PO_4)_3{\cdot}2.5H_2O$, but shrinking of the c axis was observed between 400 and 500 °C. This temperature region corresponds to the second step of weight loss in the TG curves, and no shrinking of the c axes was observed in the first step of weight loss, consistent with three-dimensional structures.

Titration of $HNb_2(OH)_2(PO_4)_3{\cdot}H_2O$ with NaOH indicated 1.8 mmol/g of acidic protons, and this amount is in good agreement with the theoretical value of 1.9 mmol/g. After the titration, the product gave an XRD pattern very similar to that of the sodium niobium phosphate. The chemical formula $HNb_2(OH)_2(PO_4)_3{\cdot}H_2O$ coincides, except for the water content, with $Nb_2(OH)_2(HPO_4)(PO_4)_2{\cdot}4.4H_2O$ proposed for a layered hydrated acid niobium phosphate by Beneke and Lagaly.[6] As mentioned above, the hydrated acid niobium phosphate obtained here has a three-dimensional structure, being different in structure with the latter compound.

The ion-exchange derivatives with *n*-alkylammonium ions of the acid niobium phosphate showed a similar dependence on m: the c axis is almost constant at $m \leq 4$ and increases abruptly at $m \geq 6$. Release of phosphorus was also observed at $m \geq 6$. However, the c axis of the derivatives with $m \geq 6$ did not clearly depend on m, so intercalation of *n*-alkylamines was attempted. The c axis of the intercalation derivatives changed with m in a manner very similar to that of the ion-exchanged derivatives of sodium niobium phosphate, although the c axis was smaller than that of the ion-exchanged derivatives from the sodium niobium phosphate.

Discussion

Structural Consideration. The resemblance of the $hk0$ reflections of $NaNb_2(OH)_2(PO_4)_3{\cdot}nH_2O$ and $NbOPO_4{\cdot}nH_2O$, as shown in Figure 1, and the formation of $NbOPO_4{\cdot}nH_2O$ from $NaNb_2(OH)_2(PO_4)_3{\cdot}nH_2O$ by treatment with acids suggest that the layered structural unit of $NbO(H_2O)PO_4$ is common to both compounds. However, in the case of $NaNb_2(OH)_2(PO_4)_3{\cdot}nH_2O$, sodium and phosphate ions are taken up into the interlayer spaces. Furthermore, as indicated by the three-dimensional character of this compound, the layers are linked with phosphate groups. Phosphoric acid can be intercalated between the layers of $NbO(H_2O)PO_4$, as reported by Beneke and Lagaly,[6] for $NbOPO_4{\cdot}2H_3PO_4{\cdot}5H_2O$. The authors also suggested the formation of $Nb_2(OH)_2(HPO_4)(PO_4)_2{\cdot}nH_2O$, in which the layers are condensed by phosphoric acid, but that compound still has a layered structure with basal spacings of 11.8 Å for the dehydrated phase and 13.3 Å for the fully hydrated phase.

A structure determination by using a single crystal assigned a primitive tetragonal lattice to $VOPO_4{\cdot}2H_2O$,[2] where the layer of $VO(H_2O)PO_4$ is stacked so as to superpose a downward octahedron above a downward one and an upward octahedron above an upward one, as seen in Figure 5a. On the other hand, as all reflections observed for $NaNb_2(OH)_2(PO_4)_3{\cdot}2.5H_2O$ satisfied the relation of $h + k + l = 2n$, the compound is considered to have a body-centered tetragonal lattice. By translation of the layers of $MO(H_2O)PO_4$ (M = V, Nb) by ($^1/_2$, $^1/_2$, 0) alternatively, a body-centered cell can be derived having the c axis doubled relative to that of the original structure (Figure 5b). This translation leads to the superposition of two apices of MO_6 octahedra along the c axis: one is a downward one on the upper layer, and the other is an upward one on the lower layer. A three-dimensional structure can be formed by linking these octahedra with a phosphate group, giving the observed P:Nb ratio of 1.5 (Figure 5c). The three-dimensional framework thus formed leaves fairly large cavities in the structure, and sodium ions and water molecules in $NaNb_2(OH)_2(PO_4)_3{\cdot}2.5H_2O$ are thought to be located within the cavities. On the other hand, the layered structure of $Nb_2(OH)_2(HPO_4)(PO_4)_2{\cdot}nH_2O$ can be formed by combining every two layers of $NbO(H_2O)PO_4$ with PO_4 in such a way that the downward octahedra are connected to downward octahedra and upward octahedra to the upward octahedra.[6]

As seen in Figure 5c, half of the c axis dimension can be approximated by adding the lengths of Nb–O, O–(P)–O (the edge of PO_4 tetrahedron), O–Nb, and Nb–O. Taking the Nb–O distance to be 2.0 Å and the edge of PO_4 to be 2.5 Å from the result of structural analysis of $NbOPO_4$[3] gives the estimated value

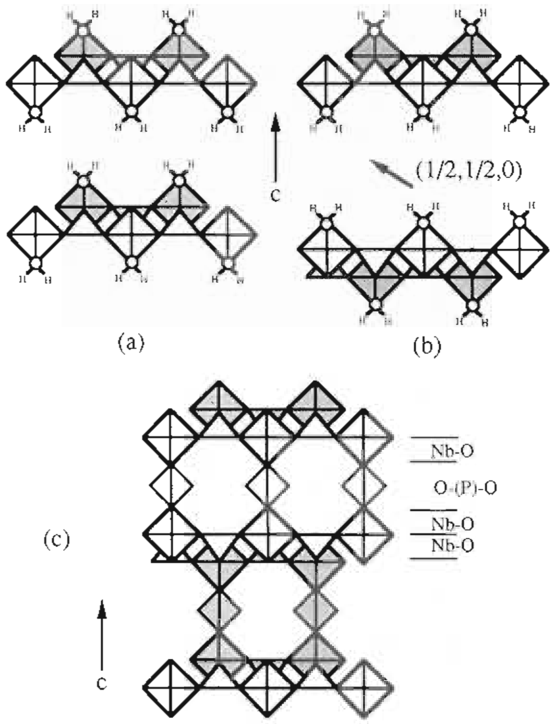

Figure 5. Schematic representation of the derivation of the structure of $NaNb_2(OH)_2(PO_4)_3 \cdot nH_2O$: (a) layered structure of $NbOPO_4 \cdot nH_2O$; (b) layers translated by ($^1/_2$, $^1/_2$, 0); (c) framework of $NaNb_2(OH)_2(PO_4)_3 \cdot nH_2O$.

2.0 × 3 + 2.5 = 8.5 Å, which agrees well with the observed value ($^{16.3}/_2$ Å). The observed density of 2.77 g/cm^3 coincides with the calculated value of 2.775 g/cm^3 for the proposed structure. Because of the lack of a single crystal, an attempt at structural determination with the powder Rietveld method[9] was carried out in the space group $I4/mmm$ and resulted in final R factors of R_{wp} = 13.0%, R_B = 12.5%, and R_P = 8.8%, indicating that the model is not far from the true structure. The fact that lower symmetry was observed for potassium niobium phosphate, the acid niobium phosphate, and the monoclinic sodium niobium phosphate at high temperature might indicate the true symmetry of tetragonal sodium niobium phosphate is lower than tetragonal.

Structural Changes with Ion Exchange and Intercalation. Sodium ions in the cavities of $NaNb_2(OH)_2(PO_4)_3 \cdot nH_2O$ and protons in acid niobium phosphate were found to be exchangeable with other alkali metal, alkaline-earth-metal, and n-alkylammonium ions. The proton is thought to be in the cavities as the hydronium ion or to be attached to the PO_4 group that links the layers. Extensive ion exchange removes not only ions in the cavities but also the PO_4 groups, and the three-dimensional structure is degraded to the two-dimensional one.

The basal spacings decreased on heating, around 100 °C for the ion-exchanged derivatives with the layered structure by loss of water and above 300 °C by loss of protons as water for the original phase and the ion-exchanged derivatives, which retain the three-dimensional structure. Figure 6 shows the minimum basal spacing observed at high temperature for each compound. The basal spacings depend linearly on the ionic radius of ions in the interlayer spaces. The three-dimensional structure is also changed to the layered structure by heating.

Organic bases are known to intercalate protonated layered compounds[10-14] but rarely to intercalate compounds with three-dimensional structures. The acid niobium phosphate can intercalate n-alkylamines in its cavities in the case of short alkyl chains and in the interlayer spaces when the chain is long. Alkylammonium ions can be also inserted by means of ion exchange. From the results of the ion exchange of sodium niobium phosphate with alkylammonium ions (Table IIb), the amount of organic ion taken up decreases with the length of alkyl chain because of the limited room of the cavities; after that, the amount of organic ion taken up begins to increase again, because the host structure is transformed to a layered structure with unlimited interlayer space by loss of the PO_4 groups connecting the layers. The basal spacings of the intercalation derivatives were smaller than the ion-exchanged derivatives at any number of carbon atoms in the chain. The increase of the basal spacing with the number of carbon atoms of 1.27 Å suggests probably a paraffin type monolayer of alkyl chains perpendicular to the layer for the ion-exchanged derivatives derived from $NaNb_2(OH)_2(PO_4)_3 \cdot nH_2O$, while a bilayer arrangement with a tilt angle of about 60° was proposed for the intercalation compounds of $NbOPO_4 \cdot nH_2O$.[6] The possible arrangements of organic ions are schematically shown in Figure 7.

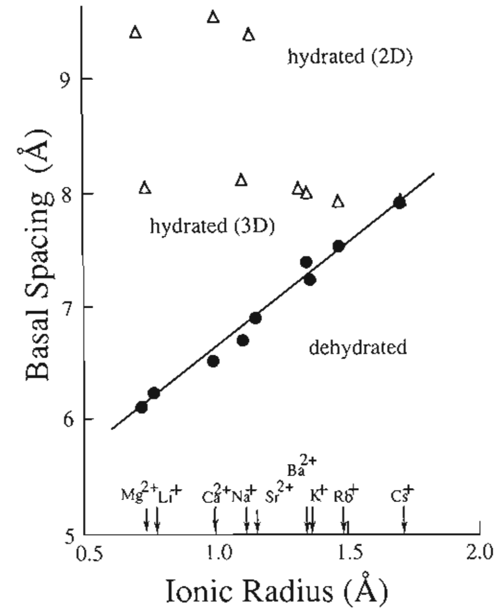

Figure 6. Minimum length of the c axis for the heat-treated compounds.

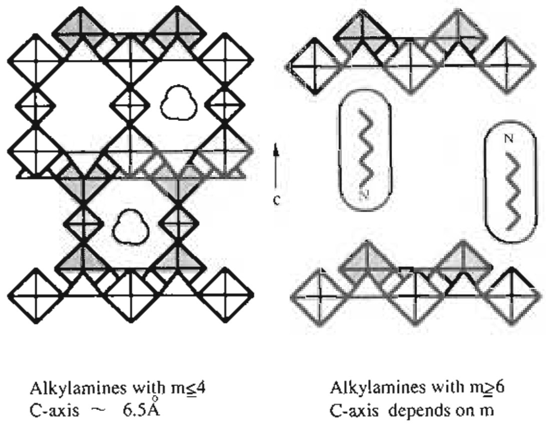

Figure 7. Possible arrangement of organic ions in the cavities (a) and interlayer spaces (b).

Conclusions

Linking the layers of $NbO(H_2O)PO_4$ by PO_4 groups leads to two structural types: one is a layered structure and the other is a three-dimensional one, having identical chemical formulas when both are acid niobium phosphates. $NbOPO_4 \cdot nH_2O$ was reported to intercalate phosphoric acid in the interlamellar spaces.[6] Compounds of the two structural types appear to be formed by

---

(9) Izumi, F. *J. Mineral. Soc. Jpn.* **1985**, *17*, 37.
(10) Michel, E.; Weiss, A. *Z. Naturforsch.* **1965**, *B20*, 1307.
(11) Rebbah, H.; Borel, M. M.; Raveau, B. *Mater. Res. Bull.* **1980**, *15*, 317.
(12) Schöllhorn, R.; Shulte-Nölle, T.; Steinhoff, G. *J. Less-Common. Met.* **1980**, *71*, 71.
(13) Lagaly, G. *Solid State Ionics* **1986**, *22*, 43.
(14) Kinomura, N.; Amano, S.; Kumada, N. *Solid State Ionics* **1990**, *37*, 317.

condensation of phosphoric acid in the interlayer spaces with the host layers in a different manner under different preparative conditions. The results obtained here indicate a possibility that compounds with various sequences of $NbO(H_2O)PO_4$ layers can be prepared by condensation with PO_4 groups and other oxoacid groups.

Acknowledgment. This research was supported by a Grant-in-Aid for Scientific Research from the Ministry of Education, Science, and Culture of Japan.

Contribution from the Chemistry Department,
University of Virginia, Charlottesville, Virginia 22901

Infrared Spectra of P_4S_{10} and Its Decomposition Products in Solid Argon

Lester Andrews,* Gregg G. Reynolds, Zofia Mielke,† and Matthew McCluskey

Received May 1, 1990

The vapor from solid molecular P_4S_{10} in a stainless steel Knudsen cell at 175 °C was trapped in solid argon for infrared spectroscopic study. Comparison with infrared spectra of solid P_4S_{10} and P_4S_9 provides a basis for identification of molecular P_4S_{10} and P_4S_9, which were isolated in comparable yields. A similar fraction of product absorptions is identified as phosphorus sulfides (PS, PS_2) and diphosphorus sulfides (P_2S_4, P_2S_5), with P_2S_5 being the major diphosphorus species in the equilibrium vapor and in superheated vapor. Photolysis of P_4S_{10} and O_3 mixtures produced new infrared absorptions for SO_2 and the terminal oxide P_4S_9O.

Introduction

Tetraphosphorus decasulfide, P_4S_{10}, was first synthesized by Berzelius in 1843 by the violent reaction of white phosphorus and sulfur, but the reaction of red phosphorus and sulfur is more controlled.[1] This compound is an important industrial chemical, used in the production of additives for lubricants, insecticides, and flotation agents.[2] Although P_4S_{10} is a molecular solid, on evaporation some of the parent molecules decompose, but apparently the decomposition is reversible because the compound may be purified by distillation.[3] The infrared spectrum of the solid has been reported by several groups,[4-7] and the Raman spectrum of the vapor (at 550 °C) is different from the solid spectrum.[6] In order to complement matrix studies of small phosphorus–sulfur transient species formed from the elements in a microwave discharge,[8] P_4S_{10} and its thermal decomposition products were trapped in solid argon for spectroscopic study.

Experimental Section

The cryogenic refrigerator, Perkin-Elmer 983 spectrometer, and vacuum apparatus have been described earlier.[9] Tetraphosphorus decasulfide, obtained from Fluka, was evaporated from a stainless steel Knudsen cell at 175–215 °C into a 2 mmol/h argon stream and condensed on a cesium iodide window maintained at 12 K. Infrared spectra were recorded from 2000 to 200 cm^{-1} on a Perkin-Elmer 983 spectrometer with sufficient resolution to give a wavenumber accuracy of ±0.5 cm^{-1}. Similar experiments were performed with a double oven, which allowed superheating of the effusing vapors in a 50-mm alumina tube 6 mm in diameter.[10]

Results

Tetraphosphorus decasulfide was evaporated from a stainless steel Knudsen cell at several temperatures. The spectrum illustrated in Figure 1 for P_4S_{10} from a 175 °C Knudsen cell contains a strong doublet at 711.3 and 707.8 cm^{-1}, three strong bands at 552.9, 540.8, and 499.2 cm^{-1}, a sharp band at 750.6 cm^{-1}, weak bands at 743.7 and 728.3 cm^{-1}, and other weaker bands listed in Table I. Also observed was a sharp trio of bands at 861.3, 765.8, and 647.7 cm^{-1} (labeled T) and a structured feature around 1000 cm^{-1}, which diminished markedly in subsequent experiments using the same sample. These latter bands arise from more volatile impurities believed to be P_4S_{10} hydrolysis products; the trio is particularly prominent in phosphine/sulfur discharge experiments where it is identified as $HSPS_2$.[11]

In the next experiment with a 185 °C cell temperature, the 707.8-cm^{-1} band was stronger than the 711.3-cm^{-1} absorption and the 540.8-cm^{-1} band was likewise stronger than the 552.9- and 499.2-cm^{-1} bands (Figure 1b). A subsequent experiment with a 215 °C cell temperature favored the 707.8- and 540.8-cm^{-1} bands even more. More sample was deposited, and a weaker band at 268.0 cm^{-1} tracked with the stronger 707.8- and 540.8-cm^{-1} bands, which are identified by arrows in Figure 1a. The 750.6- and 508.5-cm^{-1} bands were observed with the same intensity relative to each other in all of these experiments.

Table I. Infrared Absorptions (cm^{-1}) from a Sample Produced by Condensing Argon and Vapor from a 175 °C Knudsen Cell Containing Solid P_4S_{10}

absorption	identification	absorption	identification
861.3	($HSPS_2$)	552.9	P_4S_9
765.8	($HSPS_2$)	540.8	P_4S_{10}
750.6	P_2S_5	528	(P_4S_8)
748.3	P_2S_4	508.5	P_2S_5
743.7	PS_2	499.2	P_4S_9
733.3	(P_2S_4)	485.0	?
728.3	PS	460.1	?
716 sh	?	418.0	?
711.3	P_4S_9	406.2	?
707.8	P_4S_{10}	383.9	?
701	(P_4S_8)	358.9	?
647.7	($HSPS_2$)	268.0	P_4S_{10}

A similar sample was deposited from a 195 °C Knudsen cell, and 0.5-cm^{-1} resolution spectra are shown in Figure 2a. The strong 707.8- and 540.8-cm^{-1} bands dominate this spectrum. The sample was photolyzed by visible radiation (380–1000 nm) without effect, but Pyrex-filtered radiation (290–1000 nm) for 10 min decreased the 711.3-, 552.0-, and 499.2-cm^{-1} bands together, decreased the weaker 750.6-, 748.3-, and 743.7-, 733.3-, and 728.3-cm^{-1} bands, produced a new band at 716 cm^{-1}, and left the 707.8- and 540.8-cm^{-1} bands unchanged. Exposure to the full arc (220–1000 nm) for 2 min continued this trend and produced the spectrum shown in Figure 2b.

Experiments were also done by using a quartz finger to evaporate P_4S_{10} into a short tube with argon carrier gas.[8] In this case, the 750.6- and 733.3-cm^{-1} bands were much stronger than the 711.3- and 707.8-cm^{-1} bands, the 743.7-cm^{-1} absorption was observed, and the 508.5-cm^{-1} band tracked with the 750.6-cm^{-1}

---

† On leave from the University of Wroclaw, Wroclaw, Poland.

(1) Berzelius, J. *Justus Liebigs Ann. Chem.* **1843**, *46*, 251.
(2) Hoffman, H.; Becke-Goehring, M. Phosphorus Sulfides. In *Topics in Phosphorus Chemistry*; Griffith, E. J., Grayson, M., Eds.; John Wiley and Sons: New York, 1976; Vol. 8, pp 193–271.
(3) Cowley, A. H. *J. Chem. Educ.* **1964**, *41*, 530.
(4) Pitochelli, A. R.; Audrieth, L. F. *J. Am. Chem. Soc.* **1959**, *81*, 4458.
(5) Steger, E.; Blechschmidt, H. D. *Spectrochim. Acta* **1968**, *24A*, 92.
(6) Meisel, H.; Grunze, H. *Z. Anorg. Allg. Chem.* **1970**, *373*, 265.
(7) Gardner, M. *J. Chem. Soc., Dalton Trans.* **1973**, 691.
(8) Mielke, Z.; Brabson, G. D.; Andrews, L. *J. Phys. Chem.*, to be published.
(9) Andrews, L.; Withnall, R. *J. Am. Chem. Soc.* **1988**, *110*, 5605.
(10) McCluskey, M.; Andrews, L. To be published.
(11) Mielke, Z.; Andrews, L. To be published ($HSPS_2$).

0020-1669/90/1329-5222$02.50/0 © 1990 American Chemical Society